V.I. Davydenko, A.A. Ivanov, A.N. Karpushov,
R. Pozzoli, M. Romé, D.D. Ryutov

RADIAL ELECTRIC FIELD MEASUREMENT IN A TOKAMAK BY THE INJECTION OF A PULSED NEUTRAL BEAM

BUDKERINP 94-1
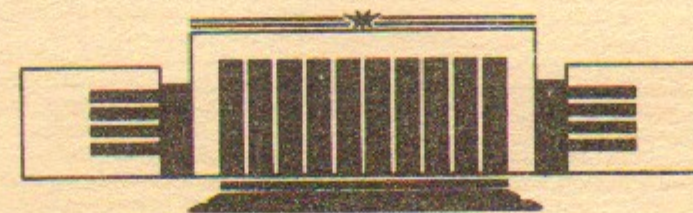
Radial Electric Field Measurement in a Tokamak by the Injection of a Pulsed Neutral Beam

V.I. Davydenko, A.A. Ivanov, A.N. Karpushov,
R. Pozzoli*, M. Romé*, D.D. Ryutov

Budker Institute of Nuclear Physics,
630090, Novosibirsk, Russia.
*Dipartimento di Fisica, Università di Milano,
Milano, Italy

The detection of the profile of the radial electric field of a tokamak by the perpendicular injection of a pulsed neutral beam into the plasma is analyzed. The method is based on the measurement of the toroidal precession velocity of the thus formed ion population. The toroidal drift is caused by the curvature of the magnetic field lines and by the electric field. For the separation of these two effects, the use of a beam with two energy fractions is studied. The application of this diagnostic scheme in a real tokamak is considered.

1   Introduction

Injection of a neutral beam (NB) to diagnose plasma parameters is widely used in controlled fusion research. The particles produced by the plasma/beam interaction give informations on the plasma density, temperature, impurity concentration, etc. Tracing of the subsequent behavior of the ions born from initial beam particles represents the essence of many of proposed schemes [1, 2, 3]. Recently, a new type of NB diagnostics has been proposed [4], based on the injection of a stack of short NB pulses (from 1 to 20 in the stack), and on the further tracing of their temporal behavior. This approach allows to localize the position of the rational magnetic surfaces and to detect the presence of the magnetic islands in tokamaks; it can also be used for the measurement of the level of microfluctuations. For these purposes, the neutral beam should be injected at a relatively small angle to the magnetic field, so as to produce the circulating ions.

It was also briefly mentioned in Ref. [4] that, by injecting the beam at large angles to the magnetic field and thereby creating bunches of toroidally trapped ions, one can provide the conditions for measuring the radial electrc field. This last issue is the object of our analysis in the present paper. We show that the measurement of the toroidal drift of an ion bunch produced by the injection of a pulsed neutral beam could provide reliable data on the profile of the radial electric field.

The paper is organized as follows. In Sec. II we describe the diagnostic scheme. In Sec. III we discuss the model used in the analysis of the motion of injected ions in a tokamak. Sec. IV contains an analysis of the requirements
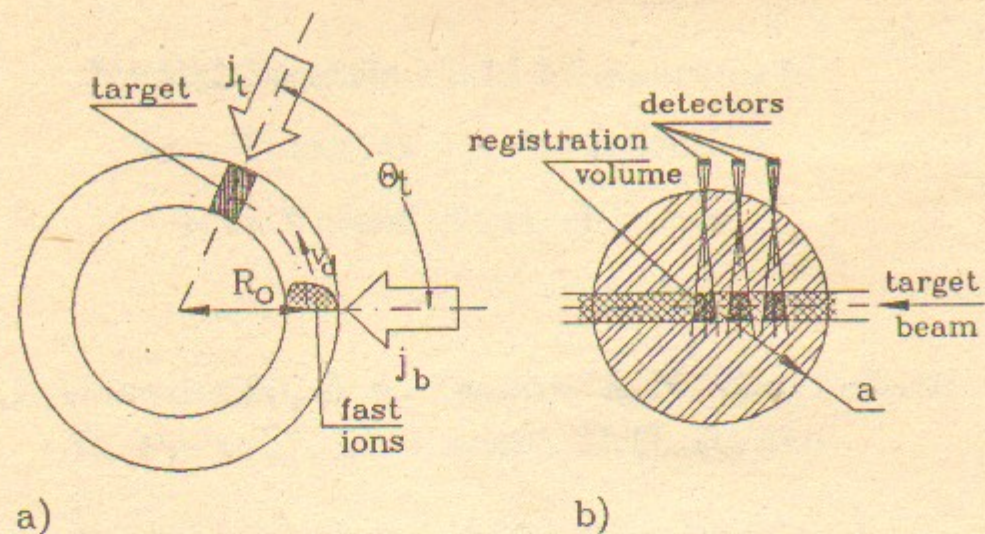
Figure 1: Diagnostic scheme.

	LBL [5]	LBL (RF) [6]	Tore supra [7]		JAERI [8]	JET [9]	
Beam species	D	H	D		D	D	T
Energy W, keV	90 120	80	72	100	95	80	80
Current I, A	58 80	25	22	40	60	53	11
Full energy, %	77 80	60	60	85	78	80	61
1/2 energy, %	12 16	30	16	10	15	10	7
1/3 energy, %	11 4	10	24	5	7	10	32

Table 1: Parameters of NB injectors.

for the parameters of diagnostic neutral beam injector and detector system. In this section we also consider a conceivable experiment with the use of this diagnostic scheme on existing tokamaks. In Sec. V is contained a review of possible approaches to development of a neutral beam injector with the required beam parameters. Sec. VI is devoted to short conclusions.

2 Description of the diagnostic scheme

For the diagnostic purpose, we suppose to inject a neutral beam into the plasma. The injection is performed perpendicularly with respect to the magnetic field, on the equatorial plane of the tokamak, from the lower field side (Fig. 1). The beam characteristics are chosen so as not to perturb the plasma parameters. Then the fast ions produced by the NB injection can be considered as test particles on a given plasma background. The produced bunch suffers a precession motion in the toroidal direction. As it will be shown in the next Section, the toroidal velocity is the sum of two parts, arising from magnetic and electric drifts. The latter part, which contains the information about the radial electric field of the tokamak is a matter of our particular interest. The parameters of this precessional motion can be obtained by measuring the density of the fast particles in one of the tokamak cross-sections. This can be done by injecting one more neutral beam into the plasma at a desired cross-section. This second neutral beam provides a charge-exchange target for the fast ions, and it is then possible to observe the thus produced charge-

exchange neutral atoms escaping from the plasma from a certain sampling volume.

As it will be shown below, for the measurement of the radial electric field, we have to be able to inject particles with two (or more) different known energies. This turns out to be the actual situation, for in every real neutral beam there is always a nonnegligible percentage of particles having only a fraction of the maximum obtainable energy, a fact that can be disturbing for many other diagnostics purposes.

As an example, in Table 1 it is shown the percentage of the different energy fractions, which are present in the NB's produced by a few existing ion sources.

3 Toroidal drift motion

Many properties of a confining toroidal system can be studied by using a model magnetic field associated with a particularly simple geometry, which retains the essential features of a real system. In the following we use for definiteness the standard model of the magnetic field of a tokamak in toroidal coordinates. This model field is not a self-consistent solution of the equation of MHD equilibrium, but it has the main advantage of being amenable to analytic treatment and is in many respects a good approximation to a realistic system. In the standard model the magnetic surfaces are simply nested concentric circular tori, and the Shafranov shift is neglected.

The toroidal coordinate system (r, ϕ, θ) is shown in Fig. 2: r is the radial coordinate, and ϕ, θ are the poloidal and toroidal angle, respectively.

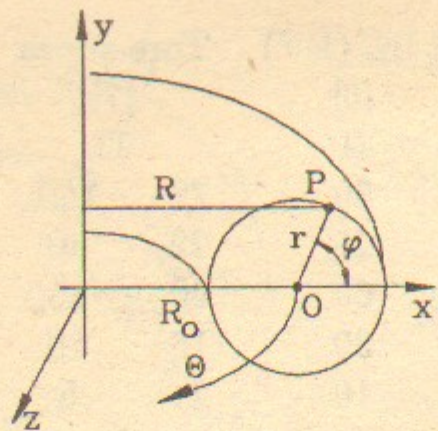The equation of the magnetic surfaces is simply given by $r = const$, and

Figure 2: Toroidal coordinate system.

the magnetic field reads

$$\mathbf{B}(r,\phi) = B_P \mathbf{e}_\phi + B_T \mathbf{e}_\theta = \frac{B_0}{q(r)}\frac{r}{R}\mathbf{e}_\phi + \frac{B_0 R_0}{R}\mathbf{e}_\theta \,, \qquad (1)$$

where B_P, B_T denote the poloidal and toroidal component of the field, respectively, R_0 represents the major radius of the torus $R = R_0 + r\cos\phi$ is the distance from the simmetry axis, B_0 is the value of $\mathbf{B}$ on the magnetic axis, and $q(r)$ is the safety factor.

Referring to a large aspect ratio tokamak, the drift motion equations for the ions, at the first order in the parameter r/R_0, read

$$\dot r = -v_{dr}\sin\phi \,; \qquad (2)$$

$$r\dot\phi = \frac{r}{qR_0}v_\parallel - v_{dr}\cos\phi + \frac{e}{m\Omega_0}\frac{d\Phi}{dr} \,; \qquad (3)$$

$$R\,\dot\theta = v_\parallel \,. \qquad (4)$$

Here we have taken into account the presence of a radial electric field, determined by the potential $\Phi(r)$, and neglected the effect of the toroidal electric field on the ion motion. In the above equations e, m are the ion charge and mass, $\Omega_0 = eB_0/mc$ is the Larmor frequency at the magnetic axis, $v_{dr} \equiv (\mu B_0/m + v_\parallel^2)/(\Omega_0 R_0)$, is the vertical drift velocity at the magnetic axis, $\mu = mv_\perp^2/2B$ the magnetic moment (assumed constant), and $v_\parallel$ is the component of the ion velocity along $\mathbf{B}$. From energy conservation it can be expressed in terms of the guiding centre coordinates:

$$v_\parallel \equiv v_\parallel(r,\phi,\mathcal{E},\mu) = \sigma\left(\frac{2}{m}[\mathcal{E} - e\Phi(r) - \mu B(r,\phi)]\right)^{1/2} \,, \qquad (5)$$

6

where $\mathcal{E}$ is the total ion energy (kinetic plus potential), and $\sigma = v_\parallel/|v_\parallel|$.

If we neglect in the first approximation the drift motion of the ions, considering only their bouncing motion along the field lines, then the radial coordinate of the guiding centre is a constant, $r = r_a$, and Eq. (4) can be written as

$$\dot\phi = \frac{\sigma}{q_a R_0}\sqrt{2(r_a/R_0)}v_{\perp a}\,\kappa\,\sqrt{1 - \frac{1}{\kappa^2}\sin^2\frac{\phi}{2}} \,, \qquad (6)$$

where the trapping parameter κ reads

$$\kappa^2 = \frac{v_{\parallel a}^2 + (r_a/R_0)v_{\perp a}^2(1 - \cos\phi_a)}{2(r_a/R_0)v_{\perp a}^2} \,. \qquad (7)$$

Here and in the following, the subscript a means the initial value.

As it is well known, it is possible to characterize two different types of trajectory, depending on the value of κ : we have trapped trajectories for $\kappa^2 < 1$, and passing trajectories for $\kappa^2 > 1$. In the following we consider only trapped particles, because this is the case we are mainly interested in, but all the computations can be easily extended to the case of passing particles.

In the case of trapped particles, the solution of Eq. (6) gives

$$\dot\phi = \frac{\sigma}{q_a R_0}\sqrt{2(r_a/R_0)}v_{\perp a}\,\kappa\,cn\left(\frac{v_{\perp a}\sqrt{r_a/R_0}}{\sqrt{2}q_a R_0}t;\kappa\right) \,, \qquad (8)$$

with $cn(\alpha;\kappa)$ the cosine Jacobian elliptic function. The bounce period can then be computed as

$$T_B = \oint\frac{d\phi}{\dot\phi} = \frac{4\sqrt{2}q_a R_0}{\sqrt{r_a/R_0}v_{\perp a}}K(\kappa) \,, \qquad (9)$$

where $K(\kappa)$ is the complete elliptic integral of the first kind.

When curvature and electric drifts are taken into account, the radial coordinate of the guiding centre is no longer a constant, and the poloidal section of the orbit has the well-known characteristic banana shape. Moreover, the bouncing motion in the poloidal direction is accompanied by a precession of the banana in the toroidal direction. The average angular velocity $<\dot\theta>$ of this precession motion can be computed by time-averaging Eq. (4) over the bounce period T_B, thus obtaining [10]

$$<\dot\theta> = \frac{q_a}{r_a}\left(v_{dr}g(\kappa) - \frac{c}{B_0}\frac{d\Phi}{dr}h(\kappa)\right) \,. \qquad (10)$$

7

The functions g, h are given by

$$g(\kappa) = 2\frac{E(\kappa)}{K(\kappa)} - 1 - \frac{r_a}{R_0}\left[1 - 2\kappa^2\frac{E(\kappa)}{K(\kappa)} + \frac{4}{3}\frac{1-(1-\kappa^2)^{3/2}}{K(\kappa)}\right]$$

$$+ 4s_a\left(\kappa^2 - 1 + \frac{E(\kappa)}{K(\kappa)}\right)$$

$$= 1 - \frac{r_a}{R_0} + \left[\frac{s_a}{2} - 1 + \left(2 - \frac{4}{\pi}\right)\frac{r_a}{R_0}\right]\kappa^2 + O(\kappa^4) ; \qquad (11)$$

$$h(\kappa) = 1 - \frac{r_a}{R_0}\left(2\frac{E(\kappa)}{K(\kappa)} - 1\right) = 1 - \frac{r_a}{R_0} + \frac{r_a}{R_0}\kappa^2 + O(\kappa^4) , \qquad (12)$$

where $E(\kappa)$ is the complete elliptic integral of the second kind, and we have introduced the shear parameter $s(r) \equiv (r/q)dq/dr$. Eq. (10) is valid under the assumption of small radial displacement. This is satisfied if $r \gg \rho_L q/(r/R_0)^{1/2}$, where ρ_L is the Larmor radius of the particle. At small $r \sim \rho_L(R_0/\rho_L)^{1/3}q^{2/3}$, a more accurate numerical computation should be required; however at such radii the method proposed here does not allow the radial detection of the electric field and is therefore not applicable. The last term in Eq. (11) which takes into account the effect of a finite radial displacement of the drift trajectory, turns to be important when the shear of the tokamak magnetic field is relatively high.

We observe that in the case of a particle injected on the equatorial plane of the tokamak perpendicularly to the magnetic field, $\kappa \ll 1$, and Eq. (10) acquires the following very simple and illustrative form

$$<\dot\theta> \simeq \frac{q_a}{r_a}\left(1 - \frac{r_a}{R_0}\right)\left(\frac{W}{m\Omega_0 R_0} + c\frac{E(r_a)}{B_0}\right) , \qquad (13)$$

where W is the kinetic energy of the ion, and $E(r) = -d\Phi/dr$ is the radial electric field. Eq.(13) is valid as far as the precession velocity evaluated from it is small as compared to the full ion velocity $(2W/M)^{1/2}$; this assumption breaks at a distance of a few ion gyroradii from the magnetic axis where, anyway, electric field becomes quite small.

The average angular velocity (13) is the sum of two terms. The first is due only to the magnetic inhomogeneity, while the second is related to the presence of the radial electric field. A measurement of the toroidal precession time at a fixed radial coordinate then allows in princile to evaluate the intensity of the electric field, if the safety factor is a known function. The knowledge of the poloidal component of the magnetic field is in fact not needed, if we are able to measure the precession times of particles with different energies. This allows to compute the electric field by means of the following very simple relationship

$$E(r_a) = \frac{W_2\tau_2 - W_1\tau_1}{eR_0(\tau_1 - \tau_2)} , \qquad (14)$$

where τ_1 (τ_2) is the precession time for a particle with energy W_1 (W_2).

The following alternative expression for the electric field strength can be derived from Eq. (13):

$$E(r_a) = \frac{r_a B_0\theta_t}{cq_a(1 - r_a/R_0)}\frac{\tau_2 W_2 - \tau_1 W_1}{\tau_1\tau_2(W_2 - W_1)} , \qquad (15)$$

where θ_t is the toroidal angular distance between injection and detection cross-sections. Only known or easily measurable quantities enter the r.h.s. of Eq. (15). This expression is useful particularly in the case $E \gg W/eR_0$, when $|\tau_1 - \tau_2| \ll \tau_1$ (see also the discussion on the accuracy of the measurement at the end of the next section).

Eq. (15) can also be written in the form

$$\frac{1}{\tau_1} - \frac{1}{\tau_2} = \frac{cq_a(1 - r_a/R_0)}{er_a B_0 R_0\theta_t}(W_1 - W_2) . \qquad (16)$$

This relationship does not contain the unknown quantity E, and can therefore be used to check the correctness of the operation of the diagnostic scheme.

Depending on the mutual orientation of the toroidal magnetic field and the toroidal current, the magnetic drift can have either the same or the opposite direction to the electric drift. In the further analysis we shall concentrate ourselves on the situation when both drifts have the same direction. The opposite case is basically the same, with the only caveat that in this case, at a certain value of the electric field, there can occur a complete compensation of the two drifts, which gives rise to very long precession times for one of the ion energies.

4   Requirements to diagnostic beam and detector array

We have studied the applicability of this method for the measurement of the radial electric field on a few modern toroidal devices whose parameters are shown in Table 2.

Parameter	TEXTOR	ASDEX	JET
Plasma major radius R_0 (cm)	175	167	296
Plasma minor radius a (cm)	46	40	210-125
Toroidal field B_0 (T)	2.25	1.2-2.45	2.7-3.45
Plasma current I (kA)	170-350	150-450	3000-4800
Safety factor q	0.5-5	0.5-7.3	1-4
Plasma density n_p ($10^{13}cm^{-3}$)	0.5-6	1.5-9	4.8-16
Electron temperature T_e (keV)	1-1.5	.8-2.5	8-13
dT/dr_{max} (eV/cm)	100	250	100
Electric field E (V/cm)	–	20-250	–
References	[11, 12, 13]	[14, 15, 16]	[17 - 20]

Table 2: Parameters of some tokamak devices.

Beam energy (keV)	σ_{ex}	σ_{ii}	$<\sigma_{ei}v_e>/v_b$	σ_{eff}
10	8.3	0.91	1.4	10.6
20	6.5	1.3	1.1	8.9
30	4.0	1.49	0.84	6.3
40	2.1	1.7	0.72	3.8
60	0.62	1.7	0.59	2.9
80	0.22	1.6	0.51	2.3
100	0.14	1.42	0.48	2

Table 3: Cross-sections ($\times 10^{-16}\ cm^2$) of relevant beam-plasma interaction processes. The data for the electron ionization process refer to $T_e = 1 keV$.

To be more specific, in the numerical examples in the following, we use the plasma parameters of TEXTOR tokamak, with a plasma density $n_p = 3 \times 10^{13} cm^{-3}$, and an electron temperature $T_e = 1 keV$. As for the radial electric field profile, we have assumed a model function of the form

$$E(r) = const\ r \exp(-r/\lambda),$$

with the parameter λ determining the position of the maximum, for which a value of $100 V/cm$ has been chosen, at a radius of $0.87a$. The angular position of the detection cross-section has been fixed at 66° after the injection cross-section.

The most important parameters of the injected beams are the energy, the current density, the pulse duration and the longitudinal and transversal width, which must be chosen in order to have a detectable signal and an accurate measurement of the electric field. The energy of the beam is related to its penetration into the plasma core. The NB attenuation is determined by the value of the effective attenuation cross-section σ_{eff}, which can be computed as

$$\sigma_{eff} = \sigma_{ex} + \sigma_{ii} + \frac{<\sigma_{ie}v_e>}{v_b} \qquad (17)$$

where σ_{ex}, σ_{ii}, σ_{ie} denote the cross-sections of the charge-exchange, proton impact and electron impact ionization process, respectively, and v_e, v_b are electron and beam particle velocities. The values of the cross-sections [21, 22] entering Eq. (17) are shown in Table 3 for the case of hydrogen target plasma and beam.

From these data it is possible to estimate that in order to obtain an appropriate attenuation length for the neutral beam, in the case of the parameters of the TEXTOR tokamak, an energy of $\sim 40 keV$ can be used.

The pulse duration of the detection beam, its longitudinal and transversal dimension, and also the dimension of the target beam must be chosen according to the requirement of an acceptable accuracy in the measurement of the intensity of the radial electric field.

If a neutral beam comprising full and half energy components is injected into the plasma, we can estimate from Eq. (15) the relative accuracy of the measurement of E by means of the following relationship

$$\frac{\Delta E}{E} = \frac{\Delta \tau}{\tau} \left(\frac{2 + \tau_2/\tau_1}{2 - \tau_2/\tau_1} + \frac{\tau_2/\tau_1 + 1}{\tau_2/\tau_1 - 1} \right), \qquad (18)$$

where the same relative accuracy on the measurement of the arrival times in the sampling volume has been assumed. In Fig. 3 the relative accuracy of the electric field measurement is shown as a function of the relative accuracy of the precession time measurement, for different values of W/eR_0E, representing the ratio between the electric and magnetic precession velocities. The relative accuracy of the measurement of the time of arrival τ is therefore a function of the required relative accuracy on the measurement of E, for given experimental conditions of the plasma, and for a given choice of the energy of the detection beam. Note that for given $\Delta\tau/\tau$ the best accuracy of the electric field measurements is attained for $W/eR_0E = \sqrt{2}$. For TEXTOR parameters this corresponds to a beam energy of a few tens of kilovolts which is consistent with the beam penetration requirements.
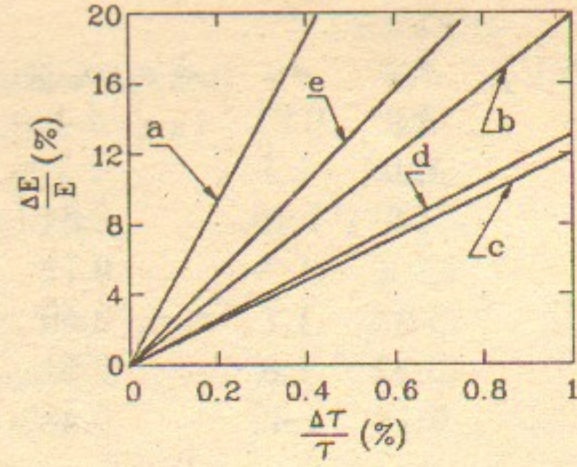
Figure 3: Relative accuracy of E *vs* relative accuracy of precession time, for different values of $W/eR_0 E$: a) 0.1, b) 0.3, c) 1, d) 3, e) 10.

Figure 4: Time of arrival of the ion for different positions of the formation point. The value $\theta = 0$ has been chosen, and the y-values (cm) are: a) 0, b) 1, c) 2, d) 3, e) 4, f) 5.

In order to provide good conditions for observing the signal, the pulse duration t_B of the diagnostic beam must be chosen according to the relationship $t_B \leq \Delta\tau$. But the pulse duration cannot be chosen arbitrary small, as it determines the number of ions in the bunch and the level of the signal in the detection system. Let y and z be the vertical and horizontal coordinate on the detection beam cross section, and L_y, L_z the corresponding widths. At small pulse lengths, the density n_f of the fast ions grows linearly with the pulse length; at pulse lengths exceeding L_z/v_D, where $v_d \simeq <\dot\theta> (R_0 + r_a)$ is the toroidal drift velocity, n_f reaches its saturation at a level $n_f \sim n_p j_{B0} \sigma_{eff} L_z / v_D$. Since L_z is assumed to be much smaller than the distance between injection and detection cross-sections, this gives a reasonable estimate on the optimal pulse duration, $t_B \simeq L_z/v_D \leq \Delta\tau$ for a given beam width.

One more effect that should be taken into account for a NB with finite longitudinal and transverse dimension is the dependence of the precession velocity on the angular coordinate ϕ and θ of the formation point. This dependence is contained in the function $g(\kappa)$ defined in Eq. (11) and is due to the dependence of the ion parallel velocity on the position of the formation point.

In Fig. 4 the time of arrival of the ion bunch is shown as a function of the minor radius, for different initial conditions of the vertical coordinate y. In Fig. 5 the same results are shown in the case of different initial conditions of the horizontal coordinate z.

From Eqs. (14), (11) we can estimate that the transversal dimension L_y of the detection beam must be chosen in order to satisfy the relationship
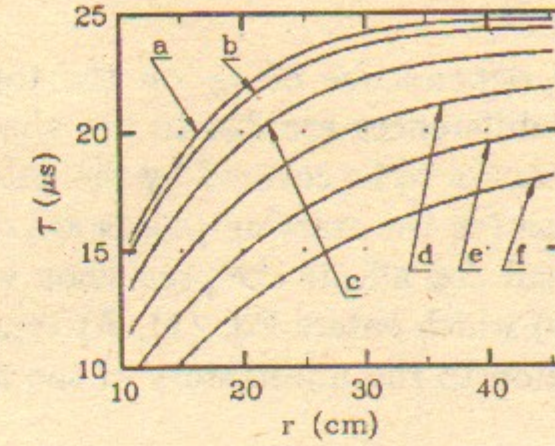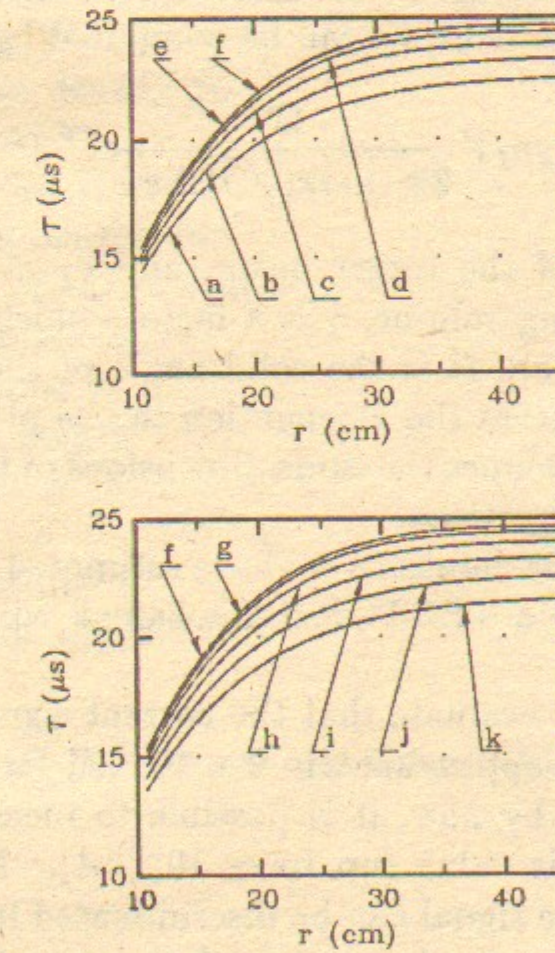

Figure 5: Time of arrival of the ion for different positions of the formation point. The ions are initially in the equatorial plane and the z-values (cm) are: a) -5, b) -4, c) -3, d) -2, e) -1, f) 0, g) 1, h) 2, i) 3, j) 4, k) 5.

$L_y \leq 2/\sqrt{|2s-1|} r (\Delta\tau/\tau)^{1/2}$.

In the latter case, the dependence of v_D on the toroidal coordinate is very weak, and the major differences are due to the above mentioned affect related to the different distances to be covered by the guiding centres in their toroidal precessional motion (as the starting points are different).

The beam angular spread $\Delta\psi$ affects the precession velocity via the term containing $v_{\|0}$ ($v_{\|0} \sim v\Delta\psi$) which enters Eq. (7). At typical angular spreads $\Delta\psi \sim 1-3^o$, its contribution to the uncertainty of the arrival time is negligibly small.

The beam energy spread ΔW causes a spread $\Delta\tau/\tau = \Delta W/W$ in the arrival time. This relationship imposes an obvious limitation on $\Delta W/W$, that seems to be not stringent because as usual stability of beam energy is better than 10^{-4}.

Let us consider now in some detail the measurements of charge-exchange flux produced by an active target. The current entering the detector system due to the charge-exchange neutrals can be computed by

$$J_r = \gamma n_f n_t \sigma_{ex} v_f V \frac{\Omega}{2\pi \cdot max[\sqrt{\Omega}; \Delta\psi]} e^{-\sigma_{eff} \int n_p dl} , \qquad (19)$$

where n_t is the density of the target beam, and v_f is the velocity of the fast ions; V is the sampling volume, γ is a factor, which takes into account the efficiency of registration, Ω is the solid angle of the analyzer, and the exponential factor arises from the attenuation in the plasma of the charge-exchange flux. Eq. (19) assumes the same dimensions of the sampling volume in poloidal and toroidal directions.

Relying upon these considerations we have estimated the parameters of a conceivable experiment in a TEXTOR-like tokamak which are summarized in Table 4.

Using Eq. (19) we can evaluate that the current signal in one channel of the registration system is approximately $2 \times 10^{-9} A$. for $\gamma = 0.9$. With the technology level achieved by now, it is possible to measure currents which are even smaller than this value (up to $\simeq 10^{-10} A$). Moreover, there are some reasons for which the signal can be discriminated from the background signal. One obvious reason is the energy of the detected particles, which is much greater than the thermal energy of the background plasma. One second reason is the very small value of the pitch angle with respect to the beam direction of the charge-exchange neutrals. This fact allows to choose for the detectors the same cross-section of injection of the target beam, and also a proper line of detection. In Fig. 6 it is shown an example of radial

Parameters of tokamak	
Poloidal field B_P	$0.2T$
Electric field E	$\simeq 100V/cm$
Accuracy of E measurement $\Delta E/E$	10%
Beam parameters	
Beam species	hydrogen
Beam energy W	$40 keV$
Beam current density j_B	$1 A cm^{-2}$
Pulse duration τ	$0.1\mu sec$
Angular spread $\Delta\psi$	$1 \div 3^o$
Target beam density n_t	$\simeq 2 \cdot 10^{10} cm^{-3}$
Parameters of experiment	
Precession angle θ_t	66°
Precession time τ	$\simeq 10\mu sec$
Attenuation length	$\simeq 80 cm$
Fast ion density n_f	$\simeq 6 \cdot 10^9 cm^{-3}$
	(at $n_e = 3 \cdot 10^{13} cm^{-3}$)
Sampling volume V	$1 \times 2.5 \times 2 cm^3$
Solid angle of analizer Ω	$2 \cdot 10^{-2} \times 5 \cdot 10^{-2}$

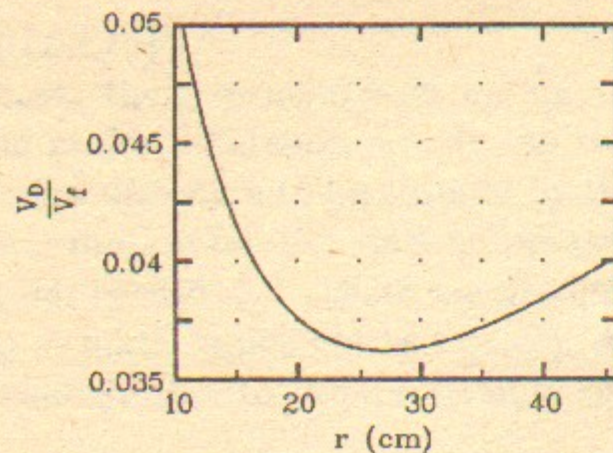Table 4: Parameters of a conceivable experiment.

Figure 6: Radial pitch angle distribution in an ion bunch.

distribution of the average pitch angle in an ion bunch. A method for better discriminate the signal can also be the use of a specie for the NB different than that of the plasma.

5 Technical feasibility analysis

There is a long history of experimental studies on the creation of hydrogen ion beams for both diagnostics and heating purposes. Technology level achieved by now undoubtedly covers the energy and current density requirements of the injector to be incorporated into the diagnostics under consideration. For example, START-2 ion source [23] developed for a pulse plasma heating would be a good candidate for this role after some redesign of the ion optics to increase the accelerating voltage. Then a problem arises how to provide a short pulse from a continuous beam. Below we will discuss a few possible approaches to that problem.

Ion beam sweeping.

One of the possible approaches could be the use of a low inductance coil system to sweep the ion beam to a small (~ 0.5 degree) angle, before the charge exchange cell. Then, initially, prior to firing the coils, neutral beam wouldn't path through the collimating slit situated well downstream from the charge-exchange cell. After firing the coils, the beam would become penetrating through the collimator. In this case the neutral beam passed through the CX cell all the time, so that there is no problem of a sudden change of the space-charge neutralization. The beam spatial deflection at a distance $\sim 0.5m$ will be only 0.5 cm, so that indeed nothing will change in the CX cell. On the contrary, in the NB duct after the cell, at a distance

2-3 m, the beam displacement will become noticeable, allowing an efficient use of the collimating system. Power supply for, say, a pair of one turn Helmholz' coils of $10cm$ radius may have roughly $2.5kA$, $5kV$ for a $100nsec$ rise time. These parameters seems to be rather routine ones. Nevertheless further experiments are required to screen limitations of this approach.

Modulation of extracting voltage.

In principle, it is possible to obtain the required parameters of the beam by fast modulation of the accelerating voltage. High voltage modulators for ion sources have a pulse front of order of a few μsec that is determined by the capacity of the ion source ($500 - 1000pF$) and the switching current available for modern switching elements ($\simeq 1kA$ per switch) [24]. We believe that a traditional scheme allows this time to be decreased to the needed value but it may be accompanied by an increased energy spread. Besides, there are also certain apprehensions that a multistage network that uses many parallel switches would be rather expensive and unreliable. Remaining are also the problems of compensation of the short ion bunch in the duct. To avoid them, one can sustain in the duct a small density plasma to compensate the beam space charge. In this respect, more attractive seems the approach that uses modulation of the plasma density inside the ion source just at the plasma grid which will be discussed below. Also possible is a partial modulation of the accelerating voltage accompanied by a further monochromatization of the beam energy (by 90 degrees bending magnet, for instance) if needed. Preliminary estimations show, that for a beam divergency of $\simeq 1^o$ it is sufficient to provide only 5% energy modulation. This version is distinguished by a reliable physics but seems to be rather complicated technically.

Modulation of plasma emitter.

Since the plasma density over the emitting surface in the ion sources is of order of $10^{12}cm^{-3}$, one can use grids with reasonable spacing and a size of the cells that subsequently repel ions and electrons to prevent the plasma entering into the accelerating structure. Potentials should be a few hundreds volts or even less for characteristic parameters of the ion source plasmas. The time of flight of the ions through the grids can be made negligible as compared to, say, $100nsec$ or less. A special negatively biased grid can be also used to absorb the ions. Similar manipulations have been already performed in the experiments described in Ref. [25]. Anyhow, further experimental efforts are needed to achieve adequate confidence in suitability of this scheme.

Pulsed stripping target.

The pulsed beam can also be realized on the basis of the negative ion source. One can use a negative ion beam instead of positive ions and neutralize the beam in a pulse photon stripping target. A negative ion source that

can provide a multi-amperes beam has been recently developed at Novosibirsk [26]. Accessibility of the photodetachment technology [27] has been already displayed in experiments of Semashko et. al. [28], who used a Nd-laser with moderate parameters. For a short pulse photoneutralizer the requirements to the laser and to the resonator's mirrors are to be even reduced. In any case, 99.5% mirror reflectivity seems not a big problem for short laser pulses. Stability of the mirror properties is high enough if the absorbed energy is less then $20 J/cm^2$. In optimal case, the photons are to move coaxially with the converted beam. The photodetachement cross section for $H^- + photon \rightarrow H^0 + e$ is $3 \times 10^{-17} cm^2$ for Nd-laser radiation [29]. Required parameters of the target can be roughly estimated if the lifetime of photons in the target is considered to be negligible comparing to the beam particles time of flight along the target. This suggestion is rather realistic since the beam velocity is much smaller then the velocity of the photons. For the sake of simplicity we also are neglecting the laser pulse duration in comparison with the photon lifetime in the target. A target length of order of $100 cm$ is adequate to provide a pulse of a few hundreds nanoseconds duration. Fraction of neutrals after the stripping is $1 - \exp(-n_{photons} \sigma_{detach} L N)$, where L is the target length and $N (\simeq 20)$ is the number of reflections from the mirrors inside the resonator. This relationship can be also rewritten in a somewhat different form suitable for estimations of required laser pulse energy [30]: $1 - \exp(-\frac{laser\ pulse\ energy}{area} \times \sigma_{detach} N/\hbar\omega)$. A target density of order of $2.7 \times 10^{13} photons/cm^3$ is sufficient to convert $\sim 80\%$ of the beam into neutrals. The total energy content in the cell with an aperture of $100 cm^2$ can be then estimated as $\sim 5.5 \times 10^{-2} J$. Lasers capable of delivering appropriate energy output with a pulse duration of $\sim 30 - 50 nsec$ are undoubtedly available. The resonator length, laser pulse duration, mirrors reflectivity and their locations should be properly chosen in order to provide the required lifetime of the target and envelope of the neutral beam pulse.

We can conclude with reasonable confidence that all the approaches, listed above, would lead to creation of an efficient diagnostic hardware. In fact, a choice among them depends on the experimental conditions and parameters to be measured with the use of this diagnostics. The approach, that uses the photon stripping, is particularly interesting because of its capability to provide very short pulses. This may be sufficient reason for the choice in certain cases. Of course, we understand that all discussed above represents only initial consideration, and it will require much more efforts, including experimental ones, to obtain reliable equipment for the experimenting.

6   Conclusions

The proposed diagnostics scheme is capable of providing an independent, direct and self-consistent determination of the radial electric field profile in a tokamak. The preliminary analysis presented in Sec. IV does not reveal any intrinsic limitations in the application of this method in medium scale tokamaks. For rather realistic assumptions regarding the diagnostic beam parameters, a 10 % uncertainty in the absolute value of the electric field is achievable. A routinely available instrumentation is required, except at most for the relatively short needed pulse duration, but the technical feasibility analysis of Sec. V demonstrates that this is not a critical issue. In comparison with another known method[31, 32] which uses an heavy ion beam, our approach displays several advantages. The most significant ones are:

1. the electric field is measured directly;

2. there is no need of differentiating the noise data;

3. a higher spatial and temporal resolution is intrinsic;

4. there is no need of scanning the beam energy;

5. an hydrogen neutral beam is more penetrant in comparison with an heavy ion beam of the same energy;

6. a simpler instrumentation is needed.

Recently, active charge-exchange recombination spectroscopy was applied to measure electric field near the plasma edge in a few large tokamaks[33, 34]. Comparing the proposed scheme to this, note that it can be used mainly on the plasma periphery and also additional data on plasma parameters from other diagnostics.

7   Acknoledgements

References

[1] R. J. Goldstone, 1984 *Principles of Plasma Physics* (Energoatomizdat, Moscow) vol. 2, p. 583 (in Russian)

[2] V. I. Davydenko, A. A. Ivanov, et al., 1896 *Plasma Diagnostics* (Energoatomizdat, Moscow), vol. 5 p. 147 (in Russian)

[3] R. J. Goldstone, Phys. Fluids **21**, 2346 (1978)

[4] D. Farina, R. Pozzoli, D. Ryutov, Plasma Phys. Control. Fusion **35**, 1243 (1993)

[5] P. D. Weber, H. M. Owren, et al., Rev. Sci. Instrum. **57**, 2714 (1986)

[6] H. Goede, et al., Rev. Sci. Instrum. **57**, 1261 (1986)

[7] P. Bayetti, R. Becher, et al., 1993 *Proc. 17th Symposium on Fusion Technology, Frascati, 1992* (ENEA, Italy), vol. 1 p. 437

[8] M. Kuriyama, Y. Ohara, et al., *ibid* p. 564

[9] P. Massman, H. D. Falter, et al., *ibid* p. 574

[10] B. B. Kadomtsev, O. P. Pogutse, Sov. Phys. JETP **24**, 1172 (1967)

[11] R. R. Weynants, D. Bora, et al., 1991 *Plasma Physics and Controlled Nuclear Fusion Research (Proc. 13th Int. Conf. Washington, 1990)* (IAEA, Vienna), vol. 1 p. 473

[12] TEXTOR Team, 1989 *Plasma Physics and Controlled Nuclear Fusion Research (Proc. 12th Int. Conf. Nice, 1988)* (IAEA, Vienna), vol. 1 p. 331

[13] J. Schluter, V. P. Bhatnagar, et al., Nucl. Fusion **5**, i065 (1985)

[14] F. Wagner, F. Ryter, et al., 1991 *Plasma Physics and Controlled Nuclear Fusion Research (Proc. 13th Int. Conf. Washington, 1990)* (IAEA, Vienna), vol. 1 p. 277

[15] M. Kaufmann, K. Behringer, et al., 1989 *Plasma Physics and Controlled Nuclear Fusion Research (Proc. 12th Int. Conf. Nice, 1988)* (IAEA, Vienna), vol. 1 p. 229

[16] ASDEX Team, Nucl. Fusion **5**, 1045 (1985)

[17] JET Team, 1991 *Plasma Physics and Controlled Nuclear Fusion Research (Proc. 13th Int. Conf. Washington, 1990)* (IAEA, Vienna) vol. 1 p. 27

[18] A. Taroni, F. Tibone, et al., *ibid* p. 93

[19] JET Team, 1989 *Plasma Physics and Controlled Nuclear Fusion Research (Proc. 12th Int. Conf. Nice, 1988)* (IAEA, Vienna), vol. 1 p. 41

[20] P. H. Rebut, R. J. Bickerton, et al., Nucl. Fusion **5**, 1011 (1985)

[21] A. C. Riviere, Nucl. Fusion **11**, 365 (1971)

[22] R. K. Janev, D. E. Post, et al., 1983 *Preprint of Princeton University PPPL-2045*

[23] V. I. Davydenko, G. V. Roslyakov, V. Ya. Savkin, Voprosy Atomnoy Nauki i Techniki, Ser. Termoyadernyi Syntez **2**, 87 (1983) (in Russian)

[24] R. Martin, et al., 1993 *Proc. 17th Symposium on Fusion Technology, Frascati, 1992* (ENEA, Italy) vol.1 p. 897

[25] J. H. Whealton, L. R. Grisham, C. C. Tsai, and W. L. Stirling, Appl. Phys. Lett. **33**, 278 (1978)

[26] Yu. I. Belchenko, G. I. Dimov, V. G. Dudnikov and A. S. Kupriyanov, Rev. Phys. Appl. **23**, 1847 (1988)

[27] J. H. Fink, 1983 *Proc. of III Symp. on Production and Neutralization of Hydrogen Ions and Beams, BNL*, p. 547

[28] W. M. Belokopytov, N. N. Semashko, P. D. Chromov, *Proc. 17th Symposium on Fusion Technology, Frascati, 1992* (ENEA, Italy), vol. 1 p. 637

[29] J. Smith, D. S. Burch, Phys. Rev. **116**, 1125 (1959)

[30] M. Bacal, G. W. Hamilton et al., Rev. Sci. Instrum. **50**, 719 (1979)

[31] J.C. Hosea, et al., Phys. Rev. Lett. **30**, (1973) p.839.

[32] K.A. Razumova, et al., Sov. JTP Lett. **7**, (1981) p.1516.

[33] E.J. Doyle, et al., Phys. Fluids Sov. **B 3(8)** Pt.2, (1991) p.2300.

[34] N. Hawkes, *Proc. 20th EPS Conference on Controlled Fusion and Plasma Physics, Lisboa, 1993* **Pt.1** (1993) Lisboa, Portugal p. 1-3.

V.I. Davydenko, A.A. Ivanov, A.N. Karpushov,
R. Pozzoli, M. Romé, D.D. Ryutov

Radial Electric Field Measurement
in a Tokamak by the Injection
of a Pulsed Neutral Beam

В.И.Давыденко, А.А. Иванов, А.Н. Карпушов,
М. Роме, Р. Поззоли, Д.Д. Рютов

Измерение радиальных электрических полей
с помощью инжекции импульсных нейтральных пучков